



Citation for published version:

Price, GJ & Shillcock, IM 2002, 'Inverse gas chromatography study of the thermodynamic behaviour of thermotropic low molar mass and polymeric liquid crystals', *Physical Chemistry Chemical Physics*, vol. 4, no. 21, pp. 5307-5316. <https://doi.org/10.1039/b202173k>

DOI:

[10.1039/b202173k](https://doi.org/10.1039/b202173k)

Publication date:

2002

Document Version

Peer reviewed version

[Link to publication](#)

University of Bath

General rights

Copyright and moral rights for the publications made accessible in the public portal are retained by the authors and/or other copyright owners and it is a condition of accessing publications that users recognise and abide by the legal requirements associated with these rights.

Take down policy

If you believe that this document breaches copyright please contact us providing details, and we will remove access to the work immediately and investigate your claim.

Inverse Gas Chromatography study of the thermodynamic behaviour of thermotropic low molar mass and polymeric liquid crystals

Gareth J. Price* and Ian M. Shillcock

Department of Chemistry, University of Bath, Claverton Down, BATH, BA2 7AY, UK.

Fax: 01225 826231. E-mail: g.j.price@bath.ac.uk

***This submission was created using the RSC Article Template (DO NOT DELETE THIS TEXT)
(LINE INCLUDED FOR SPACING ONLY - DO NOT DELETE THIS TEXT)***

We report measurements of activity coefficients and derived excess partial molar enthalpies and entropies of mixing for 17 hydrocarbon probes in three low molar mass liquid crystals as well as a polymeric version containing the same mesogenic group. Values were obtained in the isotropic liquids and in N, SmA, SmC, and N* mesophases. The results are interpreted in terms of a qualitative, descriptive model accounting for the various contributions to the energetics and the entropic effects of probe – LC interactions. The behaviour of the LC polymer was found to be determined largely by the interactions with the mesogen while the polymer backbone had a relatively minor effect.

Introduction

Thermotropic liquid crystals are compounds that show a degree of long range correlation and order in the liquid phase which changes with temperature^{1,2}. A range of mesophases can form on melting of the solid crystalline phase before an isotropic liquid forms. The least ordered of these is the nematic mesophase in which the molecules possess orientational order along a particular direction known as the director. Smectic mesophases exist where the molecules align along the director and are arranged in layers so that smectic phases are more ordered than nematics. A range of other structures is also possible. Over the past three decades or so, liquid crystal (LC) compounds have found a variety of uses and both low molar mass and polymeric versions have been developed into useful materials^{3,4,5}. Some applications, such as dyes, coatings and films utilise LC's dissolved in a solvent or dispersed in a carrier polymer. Some years ago, LC's and LC polymers, LCP's, were suggested as stationary phases for analytical gas chromatography where the molecular ordering of the LC's should allow discrimination between closely related isomeric analytes. For each of these applications, knowledge of the interactions between the components is important in designing and formulating new systems.

Inverse gas chromatography, IGC, has been used to investigate the physicochemical properties of a wide range of systems including polymers^{6,7}. While it is a dynamic method, it was shown some years ago that measurements recorded under the correct conditions could give accurate equilibrium thermodynamic information^{8,9}. The retention of an extremely small amount of a solvent or "probe" molecule in the material is recorded, the measurements being made effectively at infinite dilution of the probe. Parameters such as activity coefficients and enthalpies and entropies of solution can then be calculated.

Chow and Martire¹⁰ applied IGC to the study of a range of LC systems and developed a semi-quantitative model to describe the activity coefficients for homologous series of probe solvents in p-azoxyanisole and 4,4'-dihexoxyazoxybenzene. The model has since been applied to several LC systems^{11,12-14} and has also been applied to analytical GC systems¹⁵. A number of attempts have been made to produce a more quantitative description of LC-solvent interactions but have added little to the ability to account for the observed behaviour. For example, the model has been developed into a more rigorous statistical mechanical model based on a perturbation theory¹⁵. Bocquet and Pommier¹⁶ extended the work to finite concentration and proposed a modified retention model. Coca and co-workers¹⁷ applied the classical Flory-Huggins theory to mesophases with

non-mesomorphic probes to account for the difference in sizes of the respective molecules. However, the precise interpretation of some of the parameters involved remains open to question.

Most of the published IGC studies on LC's have evaluated thermodynamic parameters in order to characterise analytical stationary phase performance although diffusion through the various mesophases has also been considered¹⁸. The possibility of using the ordered LC structures for analytical purposes was realised some years ago and it was suggested that the best separation and column efficiency would be obtained in a nematic phase¹⁹. Kelker²⁰ first recognised that mesophases should provide good separation of geometric isomers and resolved all three xylene isomers. Since then, mesophases have been widely applied to a wide range of separations^{21,22,23}. Applications to which liquid crystal stationary phases have been applied include separations of isomers of benzene, alkanes, alkenes, heterocycles, polyaromatic hydrocarbons, polychlorinated biphenyls, and benoxaprofen isomers, as reviewed²⁴ by Witkiewicz *et al.* In parallel with the growth of polysiloxane stationary phases for a wide range of analyses, liquid crystalline versions – MEPSIL's - have been developed and a number of these materials have been studied²⁵.

One of the most commonly used and studied LC systems is the alkyl- or alkoxy- substituted cyanobiphenyls which have been widely used in display applications. Martire and co-workers^{13,11} have studied a series of alkylcyanobiphenyl molecules, characterising them in terms of activity coefficients and the associated enthalpies and entropies associated with the solution process. There have been only a few studies of LC polymers, particularly where the mesogen is attached to the polymer in a side chain^{25,26} or of main chain LCP's, where the mesogen is part of the backbone of the polymer^{27,28}. A comparison of the behaviour of siloxane-substituted cyanobiphenyls with low molar mass equivalents has been reported²⁶ briefly by Price and Shillcock and the work in this paper extends that study.

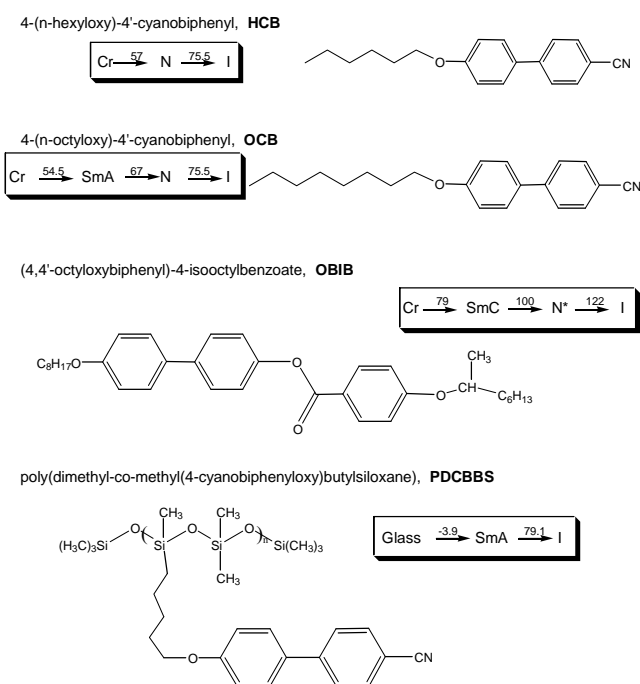
This paper presents work aimed at quantifying interactions in LC containing materials. The ability to characterise the nature and origin of the interactions between the probes and the LC's is a necessary pre-requisite to the development of new systems. Given the trends toward application and operation at high temperatures, the use of polymeric materials is preferred so that a comparison of behaviour in polymeric LC's systems with their low molar mass analogues is presented, including several previously unreported systems. We also present the first detailed comparison between low molar mass LC's and polymeric analogues.

Experimental

The liquid crystals studied were 4-(n-hexyloxy)-4'-cyanobiphenyl, HCB, 4-(n-octyloxy)-4'-cyanobiphenyl, OCB, and the polymeric poly(dimethyl-co-methyl(4-cyanobiphenoxy)butyl siloxane), PDCBBS, which had 40 repeat units. They were all supplied by Merck(UK) Ltd with reported purities of 99.5+ %. The structures are shown in Scheme 1 along with the transition temperatures and displayed mesophases reported by the manufacturers. The compounds were selected to display a range of mesophase behaviour. In Scheme 1 and the following discussion, Cr represents the solid, crystalline phase, N, SmA, SmC, and N* respectively the nematic, smectic-A, smectic-C and cholesteric (or chiral nematic) mesophases while I indicates the isotropic liquid. The poly(dimethyl siloxane), PDMS, was fractionated from a DC12500 fluid from Dow Corning and had a number average molecular weight and polydispersity of 24100 and 3.8 respectively as measured by gel permeation chromatography. All probe solvents (Aldrich Chemicals or Merck Ltd.) were 99% pure or better.

The stationary phases were prepared on acid washed, silanized Chromosorb P with 100-120 mesh size (Phase Separations). Coating was performed by slurring the LC dissolved in the minimum amount of chloroform with the support followed by removal of the solvent under rotary evaporation. After drying, 1 - 1.5 m lengths of ¼ in. o.d. copper tubing which had been washed successively with methanol, acetone and toluene were packed with a known mass of the LC coated support with the aid of a water suction pump and mechanical vibrator. The column was loaded and conditioned for 24 hr at 80 °C under a flow of carrier gas. The amount of LC or polymer on the support was determined by duplicate ashings on about 1 g of material or, for the siloxane materials, by exhaustive soxhlet extractions of a similar amount of packing with chloroform, accounting for extractable matter from the uncoated support. For HCB and OCB, loadings of 14.3 ± 0.2 % were used, the corresponding values for OBIB and PDCBBS were 8.1 ± 0.2 and 10.0 ± 0.2 %. Previous work²⁶ has shown that the support does not influence the behaviour of the LC's at this loading.

Measurements were performed on either a Pye Unicam 204 chromatograph or a Carlo Erba 400 chromatograph. Both



Scheme 1 Structures and transition temperatures (°C) of the LC stationary phases.

used oxygen-free nitrogen as the carrier gas and were fitted with FID detectors and were modified to allow accurate measurement of the inlet and outlet pressures across the column. Gas flowrates in the range of 20 – 40 cm³ min⁻¹ were used, adjusted to give retention times with appropriate accuracy. Samples of ~ 0.01 µL probe liquid and 0.4 µL of methane gas were injected by Hamilton syringe. Where baseline separation was possible several different probes were injected together. Retention times were recorded on a Hewlett Packard 3390A integrator to ± 0.01 min. Each of the values reported is the mean of at least three measurements agreeing within ± 1 % of the net retention time. To confirm the validity of using methane as the marker, the method of Peterson and Hirsch²⁹ was used to calculate the retention time due to dead space from retention measurements of three consecutive n-alkanes and values were in close agreement with those for methane retention. The column temperature was monitored to ± 0.1 °C using a thermocouple that had been calibrated against a Tinsley Type 5840 platinum resistance thermometer. The temperature variation through the oven was less than 0.2 °C. The usual checks⁷ were made to ensure that the results were independent of sample size and flow rate and that measurements were being made at conditions corresponding to infinite dilution.

Results and Discussion

Data reduction

The primary datum in IGC is the specific retention volume, V_g° , the volume of carrier gas at standard temperature and pressure (S.T.P.) per gram of stationary phase required to elute the probe³⁰. This is related to the probe retention time, t_R , by

$$V_g^\circ = \frac{(t_R - t_M)F'J}{W} \quad (1)$$

where t_M is the retention time of the methane marker, F' is the carrier flow rate corrected to S.T.P., J is the correction for gas compressibility and W the mass of stationary phase on the column. F' was calculated from the measured flow rate, F , obtained at laboratory conditions and corrected for the laboratory temperature, T , and atmospheric pressure, p_A as well as for water vapour pressure, p_w in the flow-meter using Literature constants³¹.

$$F' = F \left(\frac{273.15}{T} \right) \left(\frac{760}{p_o} \right) \left[1 - \left(\frac{p_w}{p_A} \right) \right] \quad (2)$$

The correction factor for gas compressibility is given in terms of the column inlet and outlet pressures, p_i and p_o respectively by³²

$$J = \frac{3}{2} \left[\frac{(p_i/p_o)^2 - 1}{(p_i/p_o)^3 - 1} \right] \quad (3)$$

It was shown some years ago by Everett³³ that, at infinite dilution, V_g° could be related to the thermodynamics of the probe-stationary phase interaction

$$\ln \gamma_1^\infty = \ln \left(\frac{273.15R}{V_g^\circ p_1^\circ M_2} \right) - \left(\frac{p_1^\circ (B_{11} - V_1)}{RT} \right) \quad (4)$$

where γ_1^∞ is the molar activity coefficient of the probe at infinite dilution. V_1° , B_{11} and p_1° are respectively the molar volume, the second virial coefficient and the saturated vapour pressure of the probe vapour at the column temperature T and M_2 is the relative molar mass of the stationary phase.

The activity coefficient is related to the partial molar excess Gibbs free energy of mixing, G_E and hence to the corresponding enthalpy and entropy values, H_E and S_E by

$$\ln \gamma_1^\infty = \left(\frac{\bar{G}^E}{RT} \right) = \left(\frac{\bar{H}^E}{RT} - \frac{\bar{S}^E}{R} \right) \quad (5)$$

It is also readily shown³⁰, that V_g° is related to the Gibbs free energy of solution, ΔG° , of the probe in the stationary phase by

$$\Delta G^{\text{sol}} = -RT \ln V_g^\circ - C = \Delta H^{\text{sol}} - T\Delta S^{\text{sol}} \quad (6)$$

where C is a constant dependent on the choice of reference state. For this work, it is customary to define the reference state as that of an infinitely dilute ideal vapour at 1 bar.

However, calculation of the activity coefficients presents problems when considering polymeric systems. Use of equation (4) requires knowledge of an accurate molar mass for the stationary phase component. Often this is not known for polymer solutions and all synthetic polymers pose the added problem of polydispersity in chain length. Also, early work on long chain alkane stationary phases³⁴ gave activity coefficients which became increasingly dependent on molecular mass as the chain length increased, which was at variance with the asymptotic behaviour of other physical parameters. Patterson *et al.*³⁴ circumvented this problem by introducing a weight fraction based activity coefficient, Ω , which better describes the observed behaviour of the solutions where the thermodynamic activity of the solvent, a_1 , is given by:

$$a_1 = \gamma_1 x_1 = \Omega_1 w_1 \quad (7)$$

where x and w are the mole and weight fractions of a component respectively. The weight activity coefficient has become the most widely used of these parameters in IGC of polymers and can be calculated from chromatographic data using the molar mass of the probe, M_1 and:

$$\ln \Omega_1^\infty = \ln \left(\frac{a_1}{w_1} \right)^\infty = \ln \left(\frac{273.15R}{V_g^\circ p_1^\circ M_1} \right) - \left(\frac{p_1^\circ (B_{11} - V_1)}{RT} \right) \quad (8)$$

When considering polymers, it is convenient to use the Flory-Huggins interaction parameter, χ . This represents the free energy of mixing due to other than simple combinatorial or mixing considerations. It may be calculated from:

$$\chi^\infty = \ln \Omega_1^\infty - \left(1 - \frac{V_1^\circ}{V_2^\circ} \right) + \ln \left(\frac{M_1 V_2^\circ}{M_2 V_1^\circ} \right) \quad (9)$$

In applying Equations (1) – (9), pure component data were taken from reliable Literature sources^{35,31,36,37}

The retention model

Discussion of the properties of the LC's will be given in terms of the activity coefficient (i.e. \bar{G}^E) and its enthalpic and entropic contributions. \bar{H}^E and \bar{S}^E represent the hypothetical transfer at infinite dilution of probe molecules from an ideal solution to the real solution. Thus while these quantities can be used to compare the behaviour of an individual probe between the different mesophases, they do not allow a direct comparison between different probes since the reference state contains that of the pure probe solvent. The ΔH^{sol} and ΔS^{sol} are defined in terms of a reference state of an infinitely dilute vapour at one bar³⁸ and so have a common reference state for all probes.

Following the model of Chow and Martire¹⁰ the thermodynamics of solution of the probe will be governed by a number of effects which contribute to the deviations from ideal solution behaviour and hence to γ_1^∞ and \bar{G}^E . Differences in

interaction energies between the probe and LC will lead to a potential energy contribution. Weaker probe-LC interactions relative to those in the pure components will give positive \bar{H}^E and increase γ_1^∞ . Similarly, ΔH^{sol} in these cases would be expected to be less negative than a case where the components interacted strongly. Dissolution of the probe would lead to a negative ΔS^{sol} but the additional order imposed by a mesophase structure would restrict the vibrational, rotational and conformational degrees of freedom of the probe. Thus, a less negative ΔS^{sol} and positive \bar{S}^E would be expected in the LC phases. These would also raise the value of γ_1^∞ . The size difference between the components would lead to a small volume of mixing effect (except in the polymer phases where it may be more substantial) leading to a small positive \bar{S}^E but this will generally be lower than the other factors. However, the enthalpic and entropic contributions cannot be considered separately. A strong interaction will induce ordering of the probe and hence restrict its movement, reducing the entropy so that the energetic and 'structural' factors are interrelated. Indeed, Chow and Martire demonstrated that in families of probes such as an homologous series of n-alkanes, there is a linear relation between ΔH^{sol} and ΔS^{sol} .

Thus, the overall values of the thermodynamic parameters are a complex function of these factors; a strongly interacting probe (negative ΔH^{sol} , lower γ_1^∞) will induce greater restriction on the solvent (less negative ΔS^{sol} , higher γ_1^∞). The values also contain a contribution from LC – LC interactions but this will be the same throughout. DSC measurements²⁶ show that the enthalpy differences between the SmA, N and I phases are of the order of 1 – 2 kJ mol⁻¹. Thus, large negative values of \bar{H}^E and ΔH^{sol} result from strong interactions within the solution. Large, negative entropy values indicate large restriction on conformational movement and translation in the solution which may be a result of the order imposed by the LC or of strong interactions between probe and LC. A probe which suffers great restrictions on mobility in solution but interacts weakly would have small ΔH^{sol} but large ΔS^{sol} . In this manner, the individual contributions can be determined from the overall solution behaviour.

The supercooled mesophases

Supercooling in liquid crystals, where the mesophase is retained on cooling below the equilibrium freezing point, was observed in early gas chromatography work²⁰ and supercooled mesophases have been reported³⁹ to be sufficiently stable to extend the separating range of these materials in analytical applications. This phase has usually been regarded as a continuation of the mesophase to lower temperature⁴⁰.

The effect is manifest in hysteresis of data recorded around the melting point on heating or cooling. This is illustrated in Figure 1 for HCB in terms of a plot of V_g° , calculated from Equation (1), versus temperature. On heating from room temperature, the characteristic large change in retention is observed on melting. However, on cooling, the reverse was not observed on passing through the freezing point. The supercooled region was sufficiently stable in both cases for reproducible measurements to be made. Further study revealed that the supercooled region could be divided into two parts. Between the melting point and ~ 50 °C, the retention volumes remained constant with time for at least 24-36 hr. No longer term study was undertaken and the retention volumes may well have remained constant over a much longer period of time. Below 50 °C, the retention times decreased markedly after a few minutes until they reached the values for the solid HCB. The time taken to reach the final value varied with temperature and allowed us to follow the crystallisation process⁴¹. Similar behaviour was observed for OBIB and OCB with the temperatures defining the two "supercooled regions" being 71 °C and 40 °C respectively.

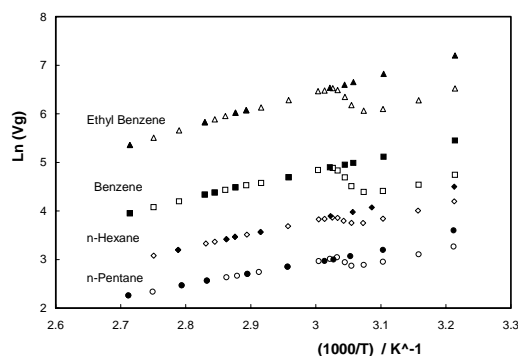


Fig.1 Retention diagram for HCB showing hysteresis* around the melting transition

* Open points – heating cycle; closed points – cooling cycle.

In Figure 1, there is a small change in slope of the plot about the N→supercooled transition suggesting that supercooled phase(s) may not simply be extensions of the mesophases to lower temperatures. However, it should be noted that there were no corresponding exotherms in the DSC thermograms and previous work in related systems has not indicated this difference in behaviour. A possible explanation for the observation is that the probe may not be sampling all of the supercooled phase leading to apparently different behaviour. In addition, these compounds have been shown to exhibit more than one solid modification⁴² and it is not clear which would form under the conditions used here. Some of the implications of the thermodynamic measurements in these supercooled mesophases will be discussed below.

Thermodynamics of interaction

Before considering the results for the individual stationary phases, some general comments regarding trends in the results are appropriate.

As the temperature increased the activity coefficient for a each probe in each phase decreased, indicating that mixing was endothermic. Generally the measured activity coefficients, calculated using Equation (4), were greater than unity indicating that the LC's were unfavourable solvents for the non-mesogenic probes. The aromatic probes exhibited lower values than the aliphatic probes indicating greater compatibility, as expected from the aromatic structure of the LC's, and γ_1^∞ for these probes became less than unity at high temperatures in the isotropic phase. This indicates that solution formation in these systems depends on the balance between unfavourable interactions between components and favourable entropy changes on mixing although these will be heavily influenced by disruption of the liquid crystal order.

The enthalpy changes accompanying transitions between phases and mesophases were shown to be small⁴¹ so that the different behaviour in each mesophase is governed by differences in probe - LC interactions and not by the changing LC - LC interactions. In addition, there is a concern that absorption of the probe will modify the LC behaviour of the stationary phase. The use of infinite dilution condition mitigates against this and the excellent agreement of mesophase transition temperatures measured for a range of LC's by IGC and other methods⁴¹ demonstrates that any modification of behaviour is not significant.

Results from other workers for three of the probes used here in HCB and OCB have been published⁴³ and show reasonable agreement with those reported here although, perhaps rather surprisingly, no mention was made of the SmA phase in the latter compound.

Hexyloxycyanobiphenyl, HCB

The molar activity coefficients at infinite dilution for a selection of probes in HCB as a function of temperature are shown in Figure 2 and the partial molar excess and solution properties listed in Tables 1 and 2. The quoted temperature is the mean value of the regression range. At least five temperatures were taken in each mesophase range although no points were taken within $\pm 1.5^\circ$ of a phase transition. There was negligible curvature in the van't Hoff plots within a particular mesophase and so the values reported are independent of temperature. The results shown below the melting point are for the supercooled N phase. Note that the values in parentheses in the tables indicate the standard deviation of the data in each mesophase, the low values indicating the general high quality of the data. A propagation of error analysis indicates that the overall uncertainty in the γ_1^∞ is $\sim 1 - 1.5\%$ and that for the enthalpy and entropy values is $\sim 4 - 6\%$.

In general the values of $\ln \gamma_1^\infty$ are positive (i.e. $\gamma_1^\infty > 1$) for the aliphatic probes indicating positive deviations from Raoult's Law and the lack of strong attractive interactions between the components. The exceptions were benzene and, at high temperatures, the other aromatic probes in the isotropic phase. That the aliphatic probes give large values indicates that the dominant interaction is with the aromatic part of the LC rather than the alkyl tail.

Consideration of the partial molar excess enthalpy values in Table 1 shows that there is little variation across the probes in the I phase, all values lying between $4.0 - 8.5 \text{ kJ mol}^{-1}$. The results for the branched alkanes were higher than their linear analogues indicating that interactions were weaker than in the linear analogue. The excess entropies for the linear alkanes were small and positive; those for the branched alkanes and the aromatic probes were rather higher, presumably as a result of the enhanced interactions.

In the N phase, the values of \overline{H}^E for an individual probe were more positive than in the I phase indicating that the interactions were weaker. This may be a result of the nematic order restricting the conformation of the probe and preventing it adopting its optimum interaction. However, the relatively weaker interactions will impose less restriction of movement on the probe so that its translational entropy will be higher. Thus, \overline{S}^E is more positive in the N phase.

Consideration of the values measured for the supercooled phase suggest them to be intermediate between those of the nematic and isotropic phases. These observations would suggest that the supercooled region was less ordered than the N phase and was able to form stronger interactions with the probe molecules. However, it is difficult to see how this could be the case and it is at variance with other published work. The observations are probably an artefact of the method resulting from the effects discussed in the previous section of this paper.

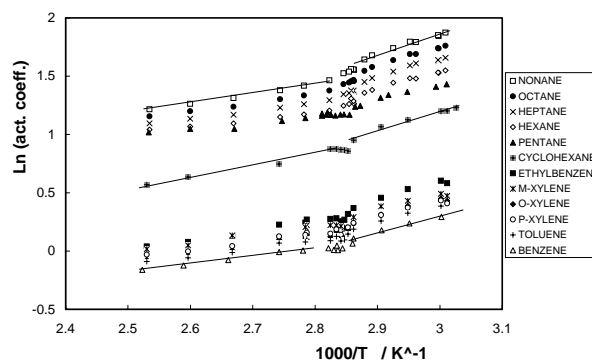


Fig. 2 Molar activity coefficients at infinite dilution for probes in HCB.

Table 1 Partial molar excess enthalpies (kJ mol^{-1}) and entropies ($\text{J mol}^{-1} \text{K}^{-1}$) at infinite dilution for probes in HCB. (Values in parentheses are the standard deviations of the plots)

Mesophase PROBE	I		N		N ^{super}	
	\overline{H}^E	\overline{S}^E	\overline{H}^E	\overline{S}^E	\overline{H}^E	\overline{S}^E
Pentane	4.0 (0.7)	1.6 (1.5)	10.4 (0.7)	13.9 (0.4)	6.3 (0.3)	6.9 (0.3)
Hexane	4.7 (0.3)	3.4 (0.7)	11.3 (0.6)	21.0 (0.7)	7.3 (1.2)	9.3 (1.2)
Heptane	5.7 (0.2)	5.5 (0.6)	11.8 (0.7)	21.8 (0.7)	8.0 (1.1)	10.3 (1.2)
Octane	6.3 (0.3)	6.4 (0.7)	12.4 (0.7)	22.8 (0.7)	8.6 (1.1)	11.2 (1.2)
Nonane	7.1 (0.3)	7.9 (0.8)	13.2 (0.7)	24.1 (0.7)	9.9 (1.6)	14.2 (1.7)
2-Methylhexane	7.9 (0.8)	10.4 (2.0)	13.3 (1.1)	25.6 (0.8)	11.5 (1.2)	20.4 (1.2)
3-Methylhexane	8.2 (0.5)	11.8 (1.4)	13.8 (1.3)	27.2 (1.0)	11.5 (1.1)	20.6 (1.1)
2,3-Dimethylpentane	8.5 (0.6)	12.9 (1.5)	13.4 (1.2)	30.9 (0.9)	10.7 (1.3)	18.3 (1.4)
2,4-Dimethylpentane	7.9 (0.6)	10.1 (1.4)	14.9 (1.2)	26.5 (0.9)	11.1 (0.8)	18.3 (0.8)
2,2,3-Trimethylbutane	8.2 (0.5)	11.9 (1.2)	13.4 (1.0)	26.1 (0.8)	11.0 (1.0)	18.9 (1.1)
Cyclohexane	8.2 (0.8)	16.1 (2.0)	10.9 (0.5)	22.7 (0.4)	9.4 (0.3)	18.2 (0.4)
Benzene	5.4 (0.2)	15.0 (0.6)	8.0 (1.2)	21.8 (1.1)	7.6 (0.7)	20.6 (0.8)
Toluene	5.7 (0.3)	15.1 (0.8)	10.0 (1.3)	27.0 (1.7)	7.3 (0.5)	19.0 (0.6)
Ethylbenzene	6.8 (0.4)	16.9 (1.0)	10.0 (1.7)	25.2 (1.6)	9.2 (0.9)	22.7 (1.1)
o-Xylene	6.3 (0.4)	16.6 (1.0)	9.1 (1.7)	23.6 (1.7)	8.5 (0.5)	21.9 (0.5)
m-Xylene	6.7 (0.2)	17.0 (1.7)	7.9 (1.4)	19.7 (1.2)	7.0 (0.9)	16.9 (0.8)
p-Xylene	5.7 (0.4)	14.6 (1.0)	8.0 (1.7)	20.7 (1.6)	7.2 (0.4)	18.3 (0.4)

Table 2 Partial molar enthalpies (kJ mol^{-1}) and entropies ($\text{J mol}^{-1} \text{K}^{-1}$) of solution at infinite dilution for probes in HCB. (Values in parentheses are the standard deviations)

Mesophase PROBE	I		N		N ^{super}	
	$-\Delta H^{\text{sol}}$	$-\Delta S^{\text{sol}}$	$-\Delta H^{\text{sol}}$	$-\Delta S^{\text{sol}}$	$-\Delta H^{\text{sol}}$	$-\Delta S^{\text{sol}}$
Pentane	18.6 (0.4)	72.2 (1.5)	16.3 (0.5)	66.4 (0.5)	19.4 (0.3)	75.9 (0.4)
Hexane	23.1 (0.2)	77.9 (0.2)	18.3 (0.7)	65.3 (0.1)	23.2 (1.2)	79.6 (1.6)
Heptane	26.6 (0.2)	81.2 (0.4)	22.5 (0.8)	70.3 (1.0)	27.3 (1.1)	84.9 (1.4)
Octane	30.5 (0.2)	85.6 (0.3)	26.5 (0.7)	75.2 (0.8)	31.5 (1.2)	90.4 (1.5)
Nonane	34.1 (0.2)	89.2 (0.4)	30.5 (0.7)	80.0 (0.9)	33.5 (1.5)	89.0 (2.0)
2-Methylhexane	22.9 (0.8)	74.0 (2.6)	19.3 (1.2)	64.0 (1.0)	21.9 (1.2)	71.8 (1.5)
3-Methylhexane	22.9 (0.7)	73.1 (1.9)	19.1 (1.4)	62.7 (1.3)	22.2 (1.1)	81.9 (1.4)
2,3-Dimethylpentane	22.3 (0.7)	71.5 (2.1)	17.4 (1.3)	58.1 (1.2)	22.4 (1.4)	73.0 (0.2)
2,4-Dimethylpentane	21.4 (0.6)	72.3 (1.9)	17.1 (1.2)	60.8 (1.1)	20.7 (0.8)	71.4 (1.1)
2,2,3-Trimethylbutane	20.8 (0.4)	69.6 (1.4)	17.0 (1.0)	59.5 (0.9)	20.1 (1.1)	68.8 (1.3)
Cyclohexane	21.3 (0.7)	67.1 (2.1)	20.3 (0.5)	65.1 (0.5)	22.5 (0.4)	72.0 (0.6)
Benzene	24.8 (0.3)	70.2 (1.1)	22.9 (1.1)	65.5 (1.1)	25.1 (0.7)	72.2 (0.9)
Toluene	28.6 (0.3)	73.8 (1.2)	25.8 (1.4)	66.5 (2.2)	29.6 (0.4)	77.7 (0.6)
Ethylbenzene	31.2 (0.4)	75.9 (1.2)	30.1 (1.7)	73.3 (1.9)	31.9 (0.8)	79.0 (1.1)
o-Xylene	33.1 (0.3)	77.6 (1.2)	32.3 (1.7)	76.2 (2.0)	33.1 (1.1)	78.5 (1.6)
m-Xylene	35.7 (1.7)	86.9 (5.4)	32.6 (1.4)	79.3 (1.5)	36.2 (1.0)	90.0 (1.2)
p-Xylene	32.7 (0.4)	78.4 (1.2)	32.2 (1.7)	77.8 (2.0)	34.1 (0.2)	83.3 (0.4)

Table 3 Partial molar excess enthalpies (kJ mol^{-1}) and entropies ($\text{J mol}^{-1} \text{K}^{-1}$) at infinite dilution for probes in OCB. (Values in parentheses are the standard deviations)

Mesophase PROBE	I		N		SmA	
	\overline{H}^E	\overline{S}^E	\overline{H}^E	\overline{S}^E	\overline{H}^E	\overline{S}^E
Pentane	8.9 (1.8)	15.7 (1.5)	9.5 (3.2)	17.3 (2.3)	1.7 (3.6)	-6.0 (1.9)
Hexane	9.7 (0.6)	17.4 (0.3)	11.5 (1.7)	22.1 (1.2)	4.4 (1.5)	1.1 (0.7)
Heptane	10.3 (1.3)	18.5 (0.2)	13.1 (1.4)	26.1 (1.0)	6.7 (1.5)	7.0 (0.7)
Octane	12.6 (0.2)	24.3 (0.2)	14.5 (1.1)	29.3 (0.8)	7.8 (1.5)	9.4 (0.7)
Nonane	10.6 (0.3)	18.4 (0.2)	16.0 (1.9)	35.5 (1.4)	8.9 (1.0)	14.9 (0.6)
2-Methylhexane	9.2 (0.5)	17.1 (0.6)	14.8 (1.6)	32.3 (1.2)	7.3 (0.6)	10.2 (0.3)
3-Methylhexane	10.8 (0.4)	21.7 (0.5)	15.2 (0.7)	33.8 (0.5)	8.4 (1.2)	13.8 (0.7)
2,3-Dimethylpentane	11.5 (0.3)	23.9 (0.2)	15.1 (1.6)	33.7 (0.8)	8.2 (0.5)	13.4 (0.3)
2,4-Dimethylpentane	11.3 (0.3)	22.5 (0.2)	13.2 (2.4)	27.3 (1.3)	7.0 (1.1)	9.2 (0.7)
2,2,3-Trimethylbutane	9.0 (0.8)	17.1 (0.9)	13.9 (0.5)	30.3 (0.2)	6.6 (1.1)	8.5 (0.7)
Cyclohexane	10.6 (1.1)	23.8 (1.2)	15.1 (1.9)	36.3 (1.4)	7.0 (0.6)	12.3 (0.3)
Benzene	5.4 (0.5)	16.3 (0.5)	12.0 (1.8)	34.1 (1.6)	4.1 (1.8)	10.8 (1.8)
Toluene	5.4 (0.6)	15.6 (0.6)	12.3 (1.8)	34.4 (1.6)	4.8 (1.3)	12.4 (1.3)
Ethylbenzene	7.7 (0.5)	20.7 (0.6)	14.2 (2.0)	38.4 (1.7)	5.8 (1.3)	13.8 (1.3)
o-Xylene	6.2 (0.6)	17.6 (0.7)	13.7 (2.0)	38.0 (1.7)	5.4 (1.3)	13.6 (1.3)
m-Xylene	6.5 (1.0)	18.1 (1.2)	11.4 (1.7)	30.9 (1.4)	6.1 (1.2)	15.2 (0.5)
p-Xylene	5.9 (1.6)	16.7 (0.7)	12.0 (1.9)	33.2 (1.7)	4.5 (1.5)	11.1 (1.5)

Table 4 Partial molar enthalpies (kJ mol^{-1}) and entropies ($\text{J mol}^{-1} \text{K}^{-1}$) of solution at infinite dilution for probes in OCB. (Values in parentheses are the standard deviations)

Mesophase PROBE	I		N		SmA	
	$-\Delta H^{\text{sol}}$	$-\Delta S^{\text{sol}}$	$-\Delta H^{\text{sol}}$	$-\Delta S^{\text{sol}}$	$-\Delta H^{\text{sol}}$	$-\Delta S^{\text{sol}}$
Pentane	14.9 (1.8)	61.5 (1.5)	15.0 (3.2)	62.0 (2.4)	21.5 (3.4)	81.5 (0.2)
Hexane	20.0 (0.9)	68.8 (0.7)	17.7 (1.8)	63.1 (0.1)	24.4 (1.7)	82.7 (1.4)
Heptane	23.0 (0.2)	70.7 (0.1)	20.7 (1.4)	64.9 (0.0)	26.9 (1.1)	83.1 (0.8)
Octane	24.9 (0.2)	69.6 (0.1)	23.9 (1.2)	67.3 (0.0)	31.2 (0.9)	88.8 (0.7)
Nonane	31.2 (0.2)	79.9 (0.2)	28.2 (1.8)	72.0 (1.7)	39.4 (1.0)	105.1 (0.7)
2-Methylhexane	21.0 (1.0)	65.8 (0.4)	17.3 (1.6)	56.0 (1.2)	18.6 (3.2)	59.4 (2.5)
3-Methylhexane	20.7 (0.5)	64.3 (0.7)	17.2 (0.7)	54.9 (0.5)	16.4 (3.5)	52.1 (2.0)
2,3-Dimethylpentane	19.6 (0.2)	61.4 (0.1)	16.8 (1.7)	54.0 (0.9)	17.4 (3.6)	55.4 (2.7)
2,4-Dimethylpentane	18.8 (1.4)	62.2 (1.2)	17.3 (2.5)	58.7 (1.3)	17.7 (3.2)	59.5 (2.6)
2,2,3-Trimethylbutane	20.3 (0.8)	65.4 (0.9)	15.2 (0.8)	51.7 (0.6)	15.8 (3.7)	53.3 (3.1)
Cyclohexane	19.4 (1.1)	60.6 (1.2)	15.6 (1.9)	50.5 (0.1)	21.8 (1.3)	68.6 (1.1)
Benzene	25.6 (0.2)	71.4 (0.4)	18.2 (1.8)	51.2 (1.4)	31.4 (0.9)	90.2 (0.6)
Toluene	29.7 (0.2)	75.6 (0.5)	22.2 (2.0)	55.2 (0.2)	33.8 (0.7)	89.4 (0.6)
Ethylbenzene	31.3 (0.2)	74.6 (0.6)	24.1 (2.2)	55.1 (0.2)	36.9 (0.8)	92.8 (0.6)
o-Xylene	33.6 (0.2)	77.8 (0.7)	25.9 (2.2)	56.8 (0.2)	38.6 (0.8)	94.0 (0.6)
m-Xylene	34.2 (0.9)	81.1 (1.7)	28.9 (0.2)	67.3 (0.1)	35.7 (1.2)	87.6 (0.6)
p-Xylene	33.8 (0.2)	80.2 (0.6)	26.6 (2.0)	60.4 (0.2)	38.7 (0.9)	96.0 (0.6)

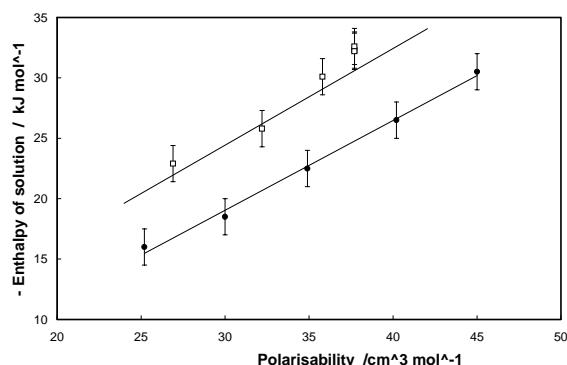


Fig. 3 Plot of the partial molar enthalpy of solution for the Nematic mesophase of HCB with n-alkane, ●, and aromatic, □, probes versus probe polarisability

In order to compare the trends between probes, the values of ΔH_{sol} and ΔS_{sol} will be considered for the reasons discussed above. For the n-alkane probes, the ability to undergo dispersion interactions increases with chain length so that ΔH_{sol} would be expected to increase (i.e. become more negative) along the series. However a more elongated molecule suffers a greater restriction in terms of translation and conformation on becoming solvated and hence ΔS_{sol} would also be expected to become more negative. This occurs in both the isotropic and the N phase of HCB. For example, in the N phase, ΔS_{sol} varied from $-66 \text{ J mol}^{-1} \text{ K}^{-1}$ for pentane to $-80 \text{ J mol}^{-1} \text{ K}^{-1}$ for nonane while ΔH_{sol} changed from $-16.3 \text{ kJ mol}^{-1}$ to $-19.3 \text{ kJ mol}^{-1}$. Figure 2 shows the activity coefficient also increases as chain length increases. Consideration of ΔH_{sol} , largely reflecting differences in potential energy, would predict that values for a given probe would increase from the isotropic phase to nematic to supercooled mesophase whereas if the restriction on probe movement were the dominant factor, the opposite trend would be predicted. The observed values indicate that the energetic term is the dominant contribution.

Comparing the results for the heptane isomers reveals similar trends to those for the n-alkanes (the former are omitted from Figure 2 for clarity but lie within the region occupied by hexane – octane). The heptane isomers present a variety of molecular shapes from the ‘globular’ 2,2,3-trimethylbutane to the ‘extended’ flexible n-heptane chain. The ΔS_{sol} decrease with the introduction of more branching in the N phase whereas there is much less variation in the I phase, reflecting the higher order in the former. A similar variation in ΔH_{sol} was noted indicating that the solution behaviour is again largely governed by the energetic interactions between probe and LC rather than restriction of the probe by the stationary phase. The number of conformations the molecule can access will decrease with branching. Thus, if the solution behaviour was governed by the potential energy difference between components, H_{sol} would follow the observed trend but the activity coefficients would exhibit the opposite trend to that observed. The trend in values for the aromatic probes was the same as for the n-alkane probes although the increase in the ΔH_{sol} and ΔS_{sol} values was smaller, reflecting the lower flexibility of the aromatic probes and hence smaller loss of degrees of freedom when dissolving in the nematic phase. In Figure 3 the ΔH_{sol} in the nematic phase are plotted as a function of probe polarisability. Similar plots were obtained for values in the two mesophases. The linear relation again suggests that the energetic interactions dominate; if there were other contributions to the potential energy, deviations from linearity in the plots would be expected.

Further insight into the effects can be gained from the C_6 probes where the polarisability increases benzene < cyclohexane < hexane while the rigidity of the molecule

increases in the opposite direction. ΔH_{sol} for benzene was more negative than that for hexane. The values for cyclohexane might be expected to fall between these two probes. This occurs in the nematic phase but not in the I liquid although the spread of values was small. Table 2 shows the ΔS_{sol} are very similar in the nematic phase for all three probes but become more positive from hexane < benzene < cyclohexane in the isotropic phase. These trends indicate a fine balance between the contributing factors to the solution behaviour as the activity coefficients are considerably different for the three probes.

Thus, our results for this LC suggest that the model which predicts that γ_1^∞ should be higher in the N phase is applicable, as has been found in most other systems that have been investigated^{13,42}.

Octyloxycyanobiphenyl, OCB

The major difference between OCB and HCB is that the two additional methylene groups extend the alkyl chain and allow a second mesophase, SmA, to form between the Cr and N phases. The molar activity coefficients for some of the probes are shown in Figure 4 and the derived enthalpies and entropies listed in Tables 3 and 4. The values for the equilibrium solid phase (i.e. those recorded on heating from room temperature) have been omitted from the figure for clarity.

The change in properties at each of the mesophase transitions is again clear. This emphasises the ability of IGC to distinguish between very small changes in the structures of the stationary phases. As with HCB, the activity coefficients reflect the change in stationary phase order as well as the temperature effect since the trend is $\gamma_1^\infty(\text{SmA})$ and $\gamma_1^\infty(\text{N}) > \gamma_1^\infty(\text{I})$.

Many of the effects observed here correspond with those seen for HCB and the discussion above will similarly apply. The nematic phase and isotropic phases exhibit identical trends to those seen in HCB. Again, the enthalpic contributions are predominant in determining the behaviour.

Although the γ_1^∞ follow a definite trend with the molecular order of the stationary phase, the same is not true for the enthalpies and entropies. The values in the SmA phase were lower (i.e. more negative or less positive) than in either of the other two phases, indicating that the strongest probe-LC interactions occur in this mesophase. Correspondingly, S_{sol} was also the least positive suggesting that the probe suffers restricted motion and conformations. This was also the case in the corresponding octyl cyanobiphenyl¹³.

Consideration of the ΔH_{sol} and ΔS_{sol} values in Table 4 shows that the results for the n-alkanes are similar to those for HCB in that longer chains result in larger potential energy interactions and greater restrictions on the probe molecule. The enthalpies and entropies could also be fitted to linear correlations with molecular polarisability, illustrating the importance of the potential energy contributions to solvation. However, the activity coefficients at all temperatures are lower than those exhibited by HCB so that OCB has a greater affinity for the

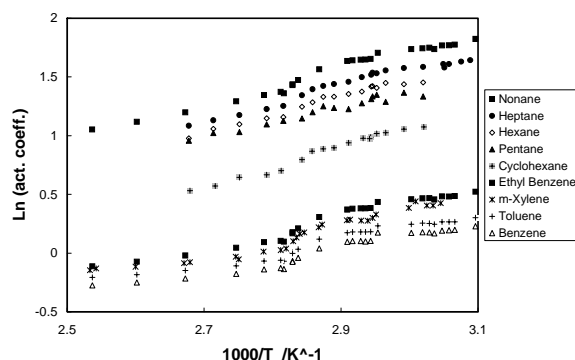


Fig. 4 Molar activity coefficients at infinite dilution for probes in OCB

probes due to the larger alkyl fragment in the LC. This behaviour is comparable to that observed in other LC systems, such as the homologous series of alkylcyanobiphenyls¹⁵ which exhibit lower activity coefficients with additional methylene units in the alkyl chain. The highest (i.e. most negative) values of ΔH_{sol} and ΔS_{sol} occur in the SmA phase while those of the N and I phases are very similar. This reflects the degree of order within the SmA phase. The probe has to enter the layered structure and also has restricted mobility; hence it loses more entropy compared with a lower order phase. In doing so, it is able to interact more effectively with the stationary phase. The same factors hold for the aromatic probes. Significantly, both the ΔH_{sol} and ΔS_{sol} for the branched alkanes and for cyclohexane are significantly lower in the SmA phase than those for the other two classes of compound. In the isotropic phase, this difference does not exist. This may indicate that the branched alkanes cannot effectively penetrate the layer structure. Computer simulation results⁴⁴ have shown that hexane will tend to adopt a longer, all-trans configuration in the smectic phase to a greater extent than in N or I phases, accounting for the result shown here.

Results for HCB and OCB showed many similarities between the two cyanobiphenyl LC's. However, the small change in structure with the longer alkyl chain in OCB had a significant influence on the interaction between probe and liquid crystal and this resulted in more favourable of solution formation over that observed in HCB. Next, we consider a LC with very different structural features.

Octyloxybiphenyl iso-octyloxybenzoate, OBIB

This molecule displays LC behaviour over a range of higher temperatures than HCB or OCB and so a more limited selection of probes was used. It displays both layered SmC and nematic phases, the latter being a chiral nematic (or cholesteric), N* phase. As far as we are aware, activity coefficients and other solution parameters in these phases have not previously been reported. The results are shown in Figure 5 and Tables 5 and 6. As in the previous case, the activity coefficients follow the degree of order in the LC, $\gamma_1^\infty(\text{SmA}) > \gamma_1^\infty(\text{N}^*) > \gamma_1^\infty(\text{I})$.

Again, the enthalpy and entropy data do not follow a simple trend. The H values in the isotropic phase are relatively small while the larger values in the mesogenic phases indicate that these are enthalpically unfavoured. In contrast to OCB, the SmC phase interacts with the probes to a lesser extent than in the isotropic liquid. H values are significantly more positive in the smectic phase of OBIB than OCB. This may be a consequence of the difference between the smectic phases (SmA phases have the molecules arranged in layers and aligned

perpendicular to the layer direction while those in the layers of a SmC phase are tilted with respect to the layer perpendicular) but is more likely related to the large alkyl fragments at each end of the molecule since the probes may interact here rather than in the ordered layers of the aromatic portions of the molecules.

For both the ΔH_{sol} and ΔS_{sol} , the cholesteric phase gave the least negative values with the alkanes whereas those in the isotropic or SmC phases are similar and around 25-30% stronger. This may suggest that the probe can interact in a similar manner in the isotropic phase or in the alkyl regions between the mesogen layers. The N* mesophase does not possess a layer structure so that in order to interact the probe must disrupt the structure. Within each phase the ΔH_{sol} for the alkanes gave a linear correlation with chain length, following the pattern seen in the previous systems where longer molecules have increased restriction of molecular flexibility and increased potential energy interactions due to the greater polarisability. The activity coefficients increased from octane to decane demonstrating the importance of the contribution of liquid crystal restriction of probe movement in a given phase.

With the aromatic probes, the N* phase again gives the lowest results but here the values in the isotropic phase are significantly higher than in either of the mesophases. Since these probes will interact with the central portion of the molecules, they must disrupt the structure in either of the mesophases. These factors would also account for the entropy values.

Poly(dimethyl-co-methyl(4-cyanobiphenoxy)butylsiloxane), PDCBBS

Having established that a rational explanation could be provided for the behaviour in low molar mass systems, we then investigated a LC polymer, also containing the cyanobiphenyl mesogen. As outlined above, activity coefficients based on mole fraction concentrations are of limited use in polymer systems. The requirement to consider weight fraction based activity coefficients, Ω_1^∞ , adds a complication to their interpretation. Figure 6 shows Ω_1^∞ values calculated using Equation (8) for the n-alkanes and two aromatic probes in HCB. Comparison with γ_1^∞ shown in Figure 2 and discussed above shows that the trend with increasing chain length has been reversed for the n-alkanes and for benzene-toluene due to the inclusion of the probe molar masses in the calculation. Thus, discussion has to take these factors into account. Similarly, excess quantities are defined in terms of an ideal solution model which will not apply_{sol} in a polymer solution. Thus, discussion will be centred on ΔH_{sol} and ΔS_{sol} .

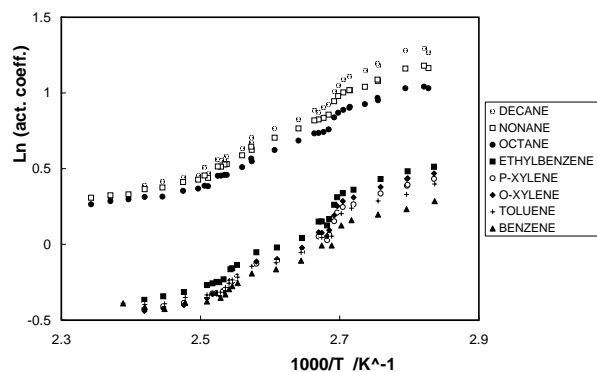


Fig. 5 Molar activity coefficients at infinite dilution for probes in OBIB

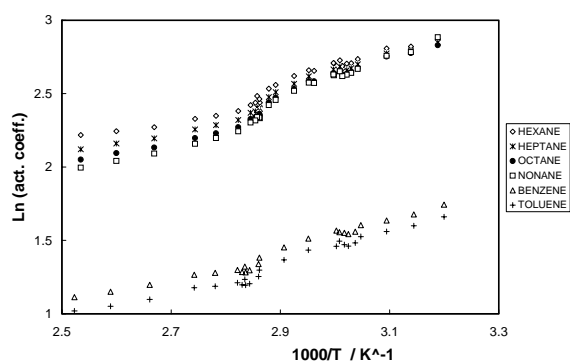


Fig. 6 Weight fraction based activity coefficients at infinite dilution for probes in HCB

Table 5 Partial molar excess enthalpies (kJ mol^{-1}) and entropies ($\text{J mol}^{-1} \text{K}^{-1}$) at infinite dilution for probes in OBIB. (Values in parentheses are the standard deviations)

Mesophase PROBE	I		N*		SmC	
	\overline{H}^E	\overline{S}^E	\overline{H}^E	\overline{S}^E	\overline{H}^E	\overline{S}^E
Octane	6.7 (0.7)	13.6 (0.7)	16.9 (1.0)	38.9 (0.9)	11.9 (0.7)	24.7 (0.8)
Nonane	8.2 (0.7)	17.0 (0.7)	17.5 (1.0)	39.7 (1.0)	13.7 (0.7)	28.9 (0.7)
Decane	8.8 (1.7)	18.1 (1.3)	18.5 (1.5)	42.0 (1.3)	16.3 (1.0)	35.2 (1.2)
Benzene	4.4 (0.7)	14.1 (0.6)	13.9 (0.4)	37.6 (0.3)	9.3 (0.7)	24.0 (0.7)
Toluene	6.1 (0.2)	18.0 (0.2)	15.0 (0.3)	40.1 (0.2)	11.4 (0.7)	29.2 (0.7)
Ethylbenzene	8.2 (0.5)	26.2 (0.5)	16.7 (0.5)	43.8 (0.5)	14.1 (0.5)	35.5 (0.7)
o-Xylene	9.5 (1.1)	26.7 (0.9)	17.4 (0.4)	46.3 (0.4)	14.9 (0.6)	38.0 (0.7)
m-Xylene	9.0 (0.8)	25.1 (0.7)	16.3 (0.7)	43.2 (0.6)	14.3 (0.6)	36.2 (0.7)
p-Xylene	8.9 (0.7)	25.1 (0.7)	15.8 (0.5)	42.2 (0.4)	15.1 (0.7)	38.9 (1.0)

Table 6 Partial molar enthalpies (kJ mol^{-1}) and entropies ($\text{J mol}^{-1} \text{K}^{-1}$) of solution at infinite dilution for probes in OBIB. (Values in parentheses are the standard deviations)

Mesophase PROBE	I		N*		SmC	
	$-\Delta H^{\text{sol}}$	$-\Delta S^{\text{sol}}$	$-\Delta H^{\text{sol}}$	$-\Delta S^{\text{sol}}$	$-\Delta H^{\text{sol}}$	$-\Delta S^{\text{sol}}$
Octane	28.1 (0.6)	77.7 (0.6)	19.3 (1.0)	56.1 (1.5)	25.6 (0.7)	73.6 (0.8)
Nonane	30.7 (0.7)	79.0 (0.7)	23.1 (1.1)	60.3 (1.0)	28.2 (0.7)	74.9 (0.9)
Decane	32.0 (1.7)	76.9 (1.7)	26.4 (1.5)	63.3 (1.2)	30.2 (1.1)	74.4 (1.2)
Benzene	27.1 (1.9)	74.3 (1.7)	14.4 (2.0)	43.0 (2.0)	22.2 (0.5)	64.9 (0.4)
Toluene	28.3 (1.4)	71.1 (1.5)	17.6 (2.1)	44.7 (2.0)	24.0 (0.7)	63.0 (0.6)
Ethylbenzene	30.4 (1.0)	75.8 (1.5)	21.7 (1.3)	50.0 (1.2)	25.3 (0.8)	61.3 (0.9)
o-Xylene	33.1 (1.1)	79.9 (1.5)	23.1 (1.6)	51.0 (1.5)	25.8 (0.7)	59.9 (0.9)
m-Xylene	31.9 (1.0)	78.5 (1.4)	22.7 (1.6)	51.7 (1.5)	25.3 (1.1)	60.1 (1.1)
p-Xylene	31.6 (1.1)	77.6 (1.5)	23.5 (1.6)	53.5 (1.5)	24.1 (0.9)	56.5 (1.0)

Table 7 Comparison of specific retention volumes ($\text{cm}^3 \text{g}^{-1}$) for PDMS at 60°C

Probe	Literature values	This work
Pentane	24.8-26.6	26.0 ± 0.3
Hexane	59.9-61.3	60.3 ± 0.8
Heptane	137.0-144.3	138.1 ± 1.5
Octane	310.6-332.1	313.1 ± 3.0
Benzene	91.6-105.5	106.8 ± 1.2
Toluene	212.8	245.6 ± 2.7
Ethylbenzene	446.1	531.0 ± 5.1
Cyclohexane	101.2-106.1	105.4 ± 1.2

Table 8 Partial molar enthalpies (kJ mol^{-1}) and entropies ($\text{J mol}^{-1} \text{K}^{-1}$) of solution at infinite dilution for probes in PDMS and PDCBBS. (Values in parentheses are the standard deviations)

PROBE	PDMS		PDCBBS SmA		PDCBBS I	
	$-\Delta H^{\text{sol}}$	$-\Delta S^{\text{sol}}$	$-\Delta H^{\text{sol}}$	$-\Delta S^{\text{sol}}$	$-\Delta H^{\text{sol}}$	$-\Delta S^{\text{sol}}$
Pentane	24.5 (0.4)	42.2 (1.4)	21.1 (1.1)	58.6 (0.9)	14.9 (2.5)	38.0 (1.8)
Hexane	28.8 (0.3)	48.2 (1.3)	25.1 (0.4)	62.7 (0.7)	19.9 (2.6)	46.8 (1.7)
Heptane	32.8 (0.3)	53.2 (1.3)	29.3 (0.4)	67.1 (1.0)	22.5 (1.0)	47.9 (0.8)
Octane	36.4 (0.6)	57.3 (1.6)	32.2 (0.7)	68.8 (1.2)	25.3 (0.5)	44.3 (1.1)
Nonane	40.3 (0.6)	62.1 (1.7)	31.7 (0.8)	56.7 (1.4)	29.6 (0.2)	56.7 (0.2)
2-Methylhexane	31.5 (0.3)	51.5 (0.6)	24.9 (1.6)	58.7 (1.5)	17.8 (1.2)	40.6 (1.0)
3-Methylhexane	31.8 (0.3)	51.7 (0.7)	26.8 (2.3)	63.3 (1.6)	19.4 (0.6)	42.1 (0.4)
2,3-Dimethylpentane	31.4 (0.2)	51.0 (0.3)	24.9 (1.9)	59.9 (1.8)	20.2 (2.5)	50.8 (2.2)
2,4-Dimethylpentane	30.2 (0.1)	50.1 (0.3)	23.5 (1.8)	58.3 (1.7)	18.3 (1.4)	45.9 (1.2)
2,2,3-Trimethylbutane	29.8 (0.2)	48.3 (0.3)	23.4 (1.6)	52.8 (2.3)	17.6 (4.3)	51.8 (1.2)
Cyclohexane	29.1 (0.2)	44.6 (0.3)	22.8 (0.9)	53.4 (0.9)	29.0 (0.0)	63.0 (1.1)
Benzene	29.4 (0.3)	45.3 (0.8)	28.8 (0.7)	61.7 (0.9)	25.3 (0.7)	56.3 (1.0)
Toluene	33.5 (0.3)	50.4 (0.8)	32.2 (0.7)	64.1 (1.0)	28.5 (0.4)	58.2 (0.8)
Ethylbenzene	37.9 (0.5)	57.5 (1.3)	34.5 (0.7)	64.1 (1.4)	30.2 (0.5)	58.9 (1.2)
o-Xylene	35.8 (0.8)	49.9 (3.2)	36.3 (0.8)	65.3 (1.6)	32.2 (0.5)	60.1 (0.9)
m-Xylene	35.3 (0.6)	49.9 (2.4)	31.4 (0.3)	57.6 (0.3)	31.8 (0.4)	57.5 (0.4)
p-Xylene	35.5 (0.7)	50.2 (2.5)	35.2 (0.8)	67.8 (0.7)	31.5 (0.6)	54.9 (0.5)

Table 9 Comparison of Flory interaction parameters for PDCBBS and OCB in the smectic and isotropic phases with PDMS

	χ^{∞} (Smectic A) (70 °C)			χ^{∞} (Isotropic) (85 °C)		
	PDCBBS	PDMS	OCB	PDCBBS	PDMS	OCB
Pentane	1.22	0.34	1.53	0.97	0.32	1.40
Hexane	1.25	0.37	1.60	0.96	0.35	1.39
Heptane	1.29	0.40	1.65	0.98	0.38	1.41
Octane	1.31	0.45	1.70	0.95	0.44	1.43
Nonane	1.29	0.51	1.71	0.97	0.50	1.45
2-Methylhexane	1.27	0.37	1.48	0.98	0.36	1.22
3-Methylhexane	1.27	0.37	1.46	0.95	0.35	1.19
2,3-Dimethylpentane	1.21	0.33	1.42	0.92	0.31	1.16
2,4-Dimethylpentane	1.30	0.34	1.49	1.02	0.32	1.26
2,2,3-Trimethylbutane	1.19	0.29	1.41	0.92	0.27	1.16
Cyclohexane	1.10	0.40	1.30	0.82	0.36	1.03
Benzene	0.57	0.54	0.59	0.27	0.44	0.31
Toluene	0.54	0.56	0.55	0.28	0.52	0.31
Ethylbenzene	0.62	0.59	0.66	0.31	0.55	0.39
p-Xylene	0.43	0.66	0.50	0.22	0.62	0.27
m-Xylene	0.57	0.70	0.57	0.24	0.66	0.30
o-Xylene	0.52	0.73	0.53	0.21	0.70	0.27

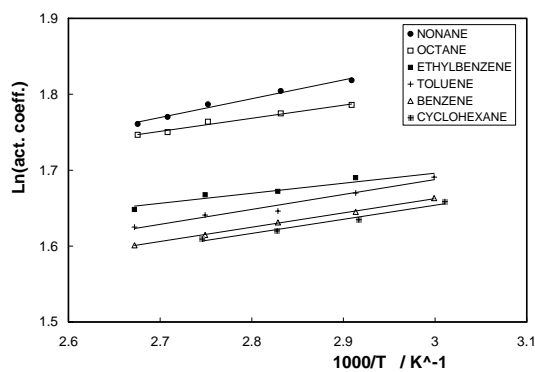


Fig. 7 Weight fraction based activity coefficients at infinite dilution for probes in PDMS

Before discussing the solution behaviour of PDCBBS, the behaviour of the same probes with PDMS was measured to ascertain the contribution of the polymer backbone. A number of studies of PDMS have been published and Table 7 compares the specific retention volumes measured at 60 °C in this work for a number of probes with Literature results. There is a large spread of results reported in the literature. Values measured in this work agreed more closely with the higher specific retention volumes reported in more recent work⁴⁵ although there was some variation with the aromatic probes.

The Ω_1^∞ for a selection of probes in PDMS are shown in Figure 7 and the expected linear dependence for a polymer well above its glass transition⁷ was observed. The ΔH^{sol} and ΔS^{sol} are listed in Table 8. Comparison of the activity coefficients with those for HCB (Figure 6) shows significant differences. PDMS distinguishes between the alkanes and the aromatics to a much greater extent; Ω_1^∞ is lower for the aromatics but higher for the alkanes in PDMS.

Consideration of the ΔH^{sol} and ΔS^{sol} values is instructive. The ΔH^{sol} results are a few kJ mol⁻¹ more negative for all probes than in HCB but significantly more than in OCB. However, the ΔS^{sol} values are all considerably lower, presumably as a result of the lower entropy of mixing associated with polymer chains. The values for the n-alkanes decrease showing more interactions as the chain length reduces. Values for the aromatic probes indicate poorer interaction with PDMS than the aliphatics as expected given the chemical nature of the polymer. The close agreement found between the xylene isomers and similarity for the heptane isomers are an indication that energetic factors dominate the solution behaviour.

The Ω_1^∞ for PDCBBS are shown in Figure 8. The glass transition temperature is well below the region studied here so the data represent the SmA phase and the isotropic polymer solution. Note that in this case, although the change of Ω_1^∞ at the phase transition is clear, it occurs over a wider temperature range than with the low molar mass materials as a result of the polydispersity of the PDCBBS. The ΔH^{sol} and ΔS^{sol} are listed in Table 7.

The general trend is that $\Omega_1^\infty(\text{I}) < \Omega_1^\infty(\text{SmA})$. The ΔH^{sol} are more negative in the SmA phase indicating stronger interactions, as was seen with the low molar mass analogue. Similarly, the ΔS^{sol} is more negative in the SmA phase. However, it is significant that the difference in ΔS^{sol} between the SmA and I phases is about 20 J K⁻¹ mol⁻¹ for the n-alkanes, lower in the branched alkanes and only around 5 – 7 J K⁻¹ mol⁻¹ for the aromatic probes. This indicates that the smectic ordering is having a greater influence on the more flexible alkanes; presumably the aromatics interact primarily with the cyanobiphenyl groups in both phases so that any difference is lower. These results suggest that the thermodynamic behaviour is largely governed by interaction with the mesogen rather than the polymer backbone. For instance, the higher activity

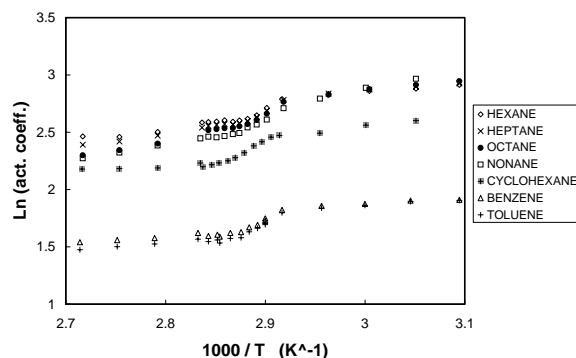


Fig. 8 Weight fraction based activity coefficients at infinite dilution for probes in PDCBBS

coefficients in the smectic phase would thus be a consequence of the entropy lost by strong interaction.

The ΔH^{sol} were of a similar magnitude to the OCB values in the SmA phase and generally considerably higher than those for PDMS. This is indicative that the mesogen was mainly controlling the solution behaviour in the mesophase with the siloxane backbone acting as a moderator to this behaviour.

In the isotropic phase the alkanes follow a linear dependence of ΔH^{sol} with polarisability as seen previously with the low molar mass materials. In the SmA phase the values also increased with rising alkyl chain length but the variation was lower and octane and nonane gave similar values. This could be a result of more restriction of the longer probe or there being no free alkyl group with which to interact, the space between mesogen and backbone not permitting the same degree of interaction. With the branched alkanes, Ω_1^∞ can be compared directly as they have the same RMM. They show that there is a complex interplay between the interaction and ordering effects but follow the same trend as in OCB and not PDMS. The entropy gain from the poorer interaction must therefore be offset

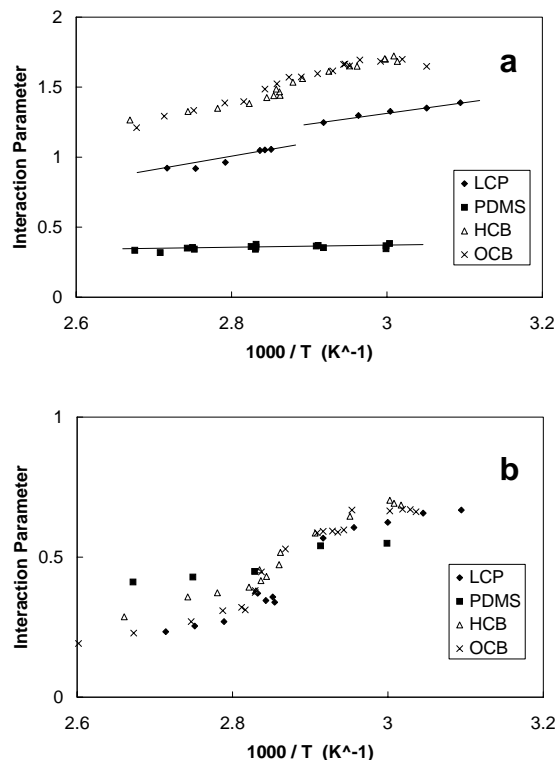


Fig. 9 Comparison of Flory interaction parameters for (a) hexane and (b) benzene in HCB, OCB, PDCBBS and PDMS.

by an entropy loss due to a more restrictive environment. This is another indication of the "tethering" effect the polysiloxane backbone has on the mesogen. The implication is a greater order in the solution. In the isotropic phase the same activity coefficient trend occurs as in the smectic phase. However, the trend in the partial molar enthalpy of solution is different. The aromatic probes generally have higher ΔH_{sol} and there was a correlation with the polarisability of the probe.

Thus, the solution behaviour of probes in the LC polymer was mainly governed by that of the mesogen and closely followed the behaviour of the low molecular mass analogue in the LC phase. However, the polymer backbone does exert some influence on the solution properties and this becomes most marked in the isotropic phase of the liquid crystal.

Further consideration of the above effects in terms of more quantitative interaction models will appear in a related publication⁴⁶. However, the dependence of properties on the mesogen can be clearly illustrated by the Flory interaction parameters, χ^∞ calculated from Equation (9). These are illustrated for two probes, n-hexane and benzene, in each of the cyanobiphenyl compounds and in the unsubstituted polymer in Figure 9. The values for the LC polymer are clearly much more related to those in the low molar mass mesogen than to PDMS. Values of the interaction parameters for all probes studied at a single temperature in each of the SmA and I phases are given in Table 9. These confirm that the behaviour is dominated by the mesogen, the effect being enhanced in the LC phase.

Conclusions

We have shown that IGC is a valuable technique for studying interactions in liquid crystalline systems. Previously published work by ourselves and other authors has been extended to a wider selection of probes in these stationary phases but also to polymeric versions of the compounds.

Using a modified version of the descriptive model of Chow and Martire, the behaviour of three low molar mass LC's with varying structures could be accounted for. In particular, the balance of the energetic and entropic contributions to the thermodynamic properties could be determined. The behaviour extended into the LC polymer where interactions were dominated by the mesogenic portion of the polymer, the siloxane backbone having a minor modifying effect on the enthalpy and entropy of solution. The results reported here can assist in interpretation of LC – solvent interactions and also have implications for the analytical performance of liquid crystalline stationary phases. This will be explored in a forthcoming publication.

Acknowledgements

We are grateful to EPSRC for the award of a Research Studentship (to IMS) and to Merck Ltd. (Poole, UK) for provision of the LC materials.

References

1. G. W. Gray, *Thermotropic liquid crystals*, Wiley, Chichester, (1987)
2. S. Chandrasekhar, *Liquid crystals*, 2nd ed, Cambridge University Press, Cambridge, (1992)
3. C. B. McArdle, *Side chain liquid crystal polymers*, Blackie, London, (1989)
4. I. C. Khoo, *Liquid crystals: physical properties and nonlinear optical phenomena* Wiley Interscience, New York, (1995)
5. P. J. Collings, *Liquid crystals: Nature's delicate phase of matter*, Hilger, Bristol, (1990)
6. D. R. Lloyd, T. C. Ward and H. P. Schreiber, (Eds.) *Inverse Gas Chromatography: Characterisation of Polymers and Other Materials ACS Symposium Series 392*, Amer. Chem. Soc., Washington DC, (1989)

7. J. E. Guillet and Z. Y. Al-Saigh, in *Encyclopedia of Analytical Chemistry: Instrumentation and Applications*, R. Meyers (Ed.), Wiley, Chichester, (2000), 7759
8. A. J. Ashworth, C. F. Chien, D. L. Furio, D. M. Hooker, M. M. Kopečni, R. J. Laub and G. J. Price, *Macromolecules*, (1984), **17**, 1090
9. W. R. Summers, Y. B. Tewari and H. P. Schreiber, *Macromolecules*, (1972), **5**, 12
10. L. C. Chow and D. E. Martire, *J. Phys. Chem.*, (1971), **75**, 2005
11. G. A. Oweimreen, G. C. Lin and D. E. Martire, *J. Phys. Chem.*, (1979), **83**, 2111
12. D. E. Martire, *J. Chromatogr.*, (1987), **406**, 27
13. S. Ghodbane, G. A. Oweimreen and D. E. Martire, *J. Chromatogr.*, (1991), **556**, 317
14. G. A. Oweimreen and A. M. AlTawfiq, *J. Chem. Eng. Data*, (1997), **42**, 996
15. D. E. Martire and C. Yan, *Anal. Chem.*, (1992), **64**, 1246
16. J. F. Bocquet and C. Pommier, *J. Chromatogr.*, (1983), **261**, 11
17. J. Coca, I. Medina and S. H. Langer, *Chromatographia*, (1988), **25**, 825
18. F. Gritti, G. Felix, M. F. Achard and F. Hardouin, *J. Chromatogr. A*, (2000), **893**, 359
19. J. E. Haky and G. M. Muschik, *J. Chromatogr.*, (1981), **214**, 161
20. H. Kelker, *Ber. Bunsenges. Phys. Chem.*, (1963), **67**, 698
21. G. M. Janini, G. M. Muschik and C. M. Hanlon, *Mol. Cryst. Liq. Cryst.*, (1979), **53**, 15
22. Z. Witkiewicz, M. Pietrzyk and R. Dabrowski, *J. Chromatogr.*, (1979), **177**, 189
23. Z. Witkiewicz, *J. Chromatogr.*, (1989), **466**, 37
24. Z. Witkiewicz and J. Mazur, *LC - GC*, (1989), **8**, 224
25. R. J. Laub, *Reference 2*, Ch. 14
26. G. J. Price and I. M. Shillcock, *Polymer*, (1993), **34**, 85
27. M. Romansky, P. F. Smith, J. E. Guillet and A. C. Griffin, *Macromolecules*, (1994), **27**, 6297
28. G. Tovar, P. J. Carreau and H. P. Schreiber, *Colloids and Surfaces A*, (2000), **161**, 213
29. M. L. Peterson and J. Hirsch, *Lipid Res.*, (1959), **1**, 132
30. J. R. Conder and C. L. Young, Wiley, New York, (1978)
31. College Station, Texas, (1965 and later revisions)
32. A. T. James and A. J. P. Martin, *Biochem. J.*, (1952), **50**, 679
33. D. H. Everett, *Trans. Farad. Soc.*, (1965), **61**, 1637
34. D. Patterson, Y. B. Tewari, H. P. Schreiber and J. E. Guillet, *Macromolecules*, (1971), **4**, 356
35. M. L. McGlashan and D. J. B. Potter, *Proc. Roy. Soc. London A*, (1962), **267**, 478
36. J. H. Dymond and E. B. Smith, *The virial coefficients of pure gases and mixtures, a critical compilation* Clarendon Press, Oxford, (1980)
37. R. C. Reid, J. M. Prausnitz and T. K. Sherwood, *The properties of gases and liquids 3rd. ed.* McGraw Hill, New York, (1977)
38. E. F. Meyer, *J. Chem. Educ.*, (1973), **50**, 191
39. M. Jawdosiuik and E. Czarnecka, *Wiad. Chem.*, (1977), **31**, 329
40. S. Wasik and S. Chester, *J. Chromatogr.*, (1976), **122**, 451
41. G. J. Price and I. M. Shillcock, *Canad. J. Chem.*, (1995), **73**, 1883
42. S.C. Jain, S.A. Agnihotry and V.G. Bhide *Mol. Cryst. Liq. Cryst.* (1982), **88**, 281
43. G. A. Oweimreen and A. K. I. Shihab, *J. Chem. Eng. Data*, (1994), **39**, 266
44. J. Alejandro, J.W. Emsley, D.J. Tildesley and P. Carlson *J. Chem. Phys.* (1994), **101**, 7027
45. M. Roth and J. Novak, *Macromolecules*, (1986), **19**, 364
46. G. J. Price and I. M. Shillcock, *Manuscripts in preparation*

Inverse Gas Chromatography study of the thermodynamic behaviour of thermotropic low molar mass and polymeric liquid crystals

Gareth J. Price* and Ian M. Shillcock

Department of Chemistry, University of Bath, Claverton Down, BATH, BA2 7AY, UK.
 Fax. 01225 826231. E-mail: g.j.price@bath.ac.uk

SUPPLEMENTARY DATA

Table S1 Partial molar excess enthalpies (kJ mol^{-1}) and entropies ($\text{J mol}^{-1} \text{K}^{-1}$) at infinite dilution for probes in OCB. (Values in parentheses are the standard deviations)

Mesophase PROBE	I		N		SmA	
	\overline{H}^E	\overline{S}^E	\overline{H}^E	\overline{S}^E	\overline{H}^E	\overline{S}^E
Pentane	8.9 (1.8)	15.7 (1.5)	9.5 (3.2)	17.3 (2.3)	1.7 (3.6)	-6.0 (1.9)
Hexane	9.7 (0.6)	17.4 (0.3)	11.5 (1.7)	22.1 (1.2)	4.4 (1.5)	1.1 (0.7)
Heptane	10.3 (1.3)	18.5 (0.2)	13.1 (1.4)	26.1 (1.0)	6.7 (1.5)	7.0 (0.7)
Octane	12.6 (0.2)	24.3 (0.2)	14.5 (1.1)	29.3 (0.8)	7.8 (1.5)	9.4 (0.7)
Nonane	10.6 (0.3)	18.4 (0.2)	16.0 (1.9)	35.5 (1.4)	8.9 (1.0)	14.9 (0.6)
2-Methylhexane	9.2 (0.5)	17.1 (0.6)	14.8 (1.6)	32.3 (1.2)	7.3 (0.6)	10.2 (0.3)
3-Methylhexane	10.8 (0.4)	21.7 (0.5)	15.2 (0.7)	33.8 (0.5)	8.4 (1.2)	13.8 (0.7)
2,3-Dimethylpentane	11.5 (0.3)	23.9 (0.2)	15.1 (1.6)	33.7 (0.8)	8.2 (0.5)	13.4 (0.3)
2,4-Dimethylpentane	11.3 (0.3)	22.5 (0.2)	13.2 (2.4)	27.3 (1.3)	7.0 (1.1)	9.2 (0.7)
2,2,3-Trimethylbutane	9.0 (0.8)	17.1 (0.9)	13.9 (0.5)	30.3 (0.2)	6.6 (1.1)	8.5 (0.7)
Cyclohexane	10.6 (1.1)	23.8 (1.2)	15.1 (1.9)	36.3 (1.4)	7.0 (0.6)	12.3 (0.3)
Benzene	5.4 (0.5)	16.3 (0.5)	12.0 (1.8)	34.1 (1.6)	4.1 (1.8)	10.8 (1.8)
Toluene	5.4 (0.6)	15.6 (0.6)	12.3 (1.8)	34.4 (1.6)	4.8 (1.3)	12.4 (1.3)
Ethylbenzene	7.7 (0.5)	20.7 (0.6)	14.2 (2.0)	38.4 (1.7)	5.8 (1.3)	13.8 (1.3)
o-Xylene	6.2 (0.6)	17.6 (0.7)	13.7 (2.0)	38.0 (1.7)	5.4 (1.3)	13.6 (1.3)
m-Xylene	6.5 (1.0)	18.1 (1.2)	11.4 (1.7)	30.9 (1.4)	6.1 (1.2)	15.2 (0.5)
p-Xylene	5.9 (1.6)	16.7 (0.7)	12.0 (1.9)	33.2 (1.7)	4.5 (1.5)	11.1 (1.5)

Table S2 Partial molar enthalpies (kJ mol^{-1}) and entropies ($\text{J mol}^{-1} \text{K}^{-1}$) of solution at infinite dilution for probes in OCB. (Values in parentheses are the standard deviations)

PROBE	Mesophase	I		N		SmA	
		$-\Delta H^{\text{sol}}$	$-\Delta S^{\text{sol}}$	$-\Delta H^{\text{sol}}$	$-\Delta S^{\text{sol}}$	$-\Delta H^{\text{sol}}$	$-\Delta S^{\text{sol}}$
Pentane		14.9 (1.8)	61.5 (1.5)	15.0 (3.2)	62.0 (2.4)	21.5 (3.4)	81.5 (0.2)
Hexane		20.0 (0.9)	68.8 (0.7)	17.7 (1.8)	63.1 (0.1)	24.4 (1.7)	82.7 (1.4)
Heptane		23.0 (0.2)	70.7 (0.1)	20.7 (1.4)	64.9 (0.0)	26.9 (1.1)	83.1 (0.8)
Octane		24.9 (0.2)	69.6 (0.1)	23.9 (1.2)	67.3 (0.0)	31.2 (0.9)	88.8 (0.7)
Nonane		31.2 (0.2)	79.9 (0.2)	28.2 (1.8)	72.0 (1.7)	39.4 (1.0)	105.1 (0.7)
2-Methylhexane		21.0 (1.0)	65.8 (0.4)	17.3 (1.6)	56.0 (1.2)	18.6 (3.2)	59.4 (2.5)
3-Methylhexane		20.7 (0.5)	64.3 (0.7)	17.2 (0.7)	54.9 (0.5)	16.4 (3.5)	52.1 (2.0)
2,3-Dimethylpentane		19.6 (0.2)	61.4 (0.1)	16.8 (1.7)	54.0 (0.9)	17.4 (3.6)	55.4 (2.7)
2,4-Dimethylpentane		18.8 (1.4)	62.2 (1.2)	17.3 (2.5)	58.7 (1.3)	17.7 (3.2)	59.5 (2.6)
2,2,3-Trimethylbutane		20.3 (0.8)	65.4 (0.9)	15.2 (0.8)	51.7 (0.6)	15.8 (3.7)	53.3 (3.1)
Cyclohexane		19.4 (1.1)	60.6 (1.2)	15.6 (1.9)	50.5 (0.1)	21.8 (1.3)	68.6 (1.1)
Benzene		25.6 (0.2)	71.4 (0.4)	18.2 (1.8)	51.2 (1.4)	31.4 (0.9)	90.2 (0.6)
Toluene		29.7 (0.2)	75.6 (0.5)	22.2 (2.0)	55.2 (0.2)	33.8 (0.7)	89.4 (0.6)
Ethylbenzene		31.3 (0.2)	74.6 (0.6)	24.1 (2.2)	55.1 (0.2)	36.9 (0.8)	92.8 (0.6)
o-Xylene		33.6 (0.2)	77.8 (0.7)	25.9 (2.2)	56.8 (0.2)	38.6 (0.8)	94.0 (0.6)
m-Xylene		34.2 (0.9)	81.1 (1.7)	28.9 (0.2)	67.3 (0.1)	35.7 (1.2)	87.6 (0.6)
p-Xylene		33.8 (0.2)	80.2 (0.6)	26.6 (2.0)	60.4 (0.2)	38.7 (0.9)	96.0 (0.6)

Table S3 Partial molar excess enthalpies (kJ mol^{-1}) and entropies ($\text{J mol}^{-1} \text{K}^{-1}$) at infinite dilution for probes in OBIB. (Values in parentheses are the standard deviations)

PROBE	Mesophase I		N*		SmC	
	\overline{H}^E	\overline{S}^E	\overline{H}^E	\overline{S}^E	\overline{H}^E	\overline{S}^E
Octane	6.7 (0.7)	13.6 (0.7)	16.9 (1.0)	38.9 (0.9)	11.9 (0.7)	24.7 (0.8)
Nonane	8.2 (0.7)	17.0 (0.7)	17.5 (1.0)	39.7 (1.0)	13.7 (0.7)	28.9 (0.7)
Decane	8.8 (1.7)	18.1 (1.3)	18.5 (1.5)	42.0 (1.3)	16.3 (1.0)	35.2 (1.2)
Benzene	4.4 (0.7)	14.1 (0.6)	13.9 (0.4)	37.6 (0.3)	9.3 (0.7)	24.0 (0.7)
Toluene	6.1 (0.2)	18.0 (0.2)	15.0 (0.3)	40.1 (0.2)	11.4 (0.7)	29.2 (0.7)
Ethylbenzene	8.2 (0.5)	26.2 (0.5)	16.7 (0.5)	43.8 (0.5)	14.1 (0.5)	35.5 (0.7)
o-Xylene	9.5 (1.1)	26.7 (0.9)	17.4 (0.4)	46.3 (0.4)	14.9 (0.6)	38.0 (0.7)
m-Xylene	9.0 (0.8)	25.1 (0.7)	16.3 (0.7)	43.2 (0.6)	14.3 (0.6)	36.2 (0.7)
p-Xylene	8.9 (0.7)	25.1 (0.7)	15.8 (0.5)	42.2 (0.4)	15.1 (0.7)	38.9 (1.0)

Table S4 Partial molar enthalpies (kJ mol^{-1}) and entropies ($\text{J mol}^{-1} \text{K}^{-1}$) of solution at infinite dilution for probes in OBIB. (Values in parentheses are the standard deviations)

Mesophase PROBE	I		N*		SmC	
	$-\Delta H^{\text{sol}}$	$-\Delta S^{\text{sol}}$	$-\Delta H^{\text{sol}}$	$-\Delta S^{\text{sol}}$	$-\Delta H^{\text{sol}}$	$-\Delta S^{\text{sol}}$
Octane	28.1 (0.6)	77.7 (0.6)	19.3 (1.0)	56.1 (1.5)	25.6 (0.7)	73.6 (0.8)
Nonane	30.7 (0.7)	79.0 (0.7)	23.1 (1.1)	60.3 (1.0)	28.2 (0.7)	74.9 (0.9)
Decane	32.0 (1.7)	76.9 (1.7)	26.4 (1.5)	63.3 (1.2)	30.2 (1.1)	74.4 (1.2)
Benzene	27.1 (1.9)	74.3 (1.7)	14.4 (2.0)	43.0 (2.0)	22.2 (0.5)	64.9 (0.4)
Toluene	28.3 (1.4)	71.1 (1.5)	17.6 (2.1)	44.7 (2.0)	24.0 (0.7)	63.0 (0.6)
Ethylbenzene	30.4 (1.0)	75.8 (1.5)	21.7 (1.3)	50.0 (1.2)	25.3 (0.8)	61.3 (0.9)
o-Xylene	33.1 (1.1)	79.9 (1.5)	23.1 (1.6)	51.0 (1.5)	25.8 (0.7)	59.9 (0.9)
m-Xylene	31.9 (1.0)	78.5 (1.4)	22.7 (1.6)	51.7 (1.5)	25.3 (1.1)	60.1 (1.1)
p-Xylene	31.6 (1.1)	77.6 (1.5)	23.5 (1.6)	53.5 (1.5)	24.1 (0.9)	56.5 (1.0)

Table S5 Partial molar enthalpies (kJ mol^{-1}) and entropies ($\text{J mol}^{-1} \text{K}^{-1}$) of solution at infinite dilution for probes in PDMS and PDCBBS. (Values in parentheses are the standard deviations)

PROBE	PDMS		PDCBBS SmA		PDCBBS I	
	$-\Delta H^{\text{sol}}$	$-\Delta S^{\text{sol}}$	$-\Delta H^{\text{sol}}$	$-\Delta S^{\text{sol}}$	$-\Delta H^{\text{sol}}$	$-\Delta S^{\text{sol}}$
Pentane	24.5 (0.4)	42.2 (1.4)	21.1 (1.1)	58.6 (0.9)	14.9 (2.5)	38.0 (1.8)
Hexane	28.8 (0.3)	48.2 (1.3)	25.1 (0.4)	62.7 (0.7)	19.9 (2.6)	46.8 (1.7)
Heptane	32.8 (0.3)	53.2 (1.3)	29.3 (0.4)	67.1 (1.0)	22.5 (1.0)	47.9 (0.8)
Octane	36.4 (0.6)	57.3 (1.6)	32.2 (0.7)	68.8 (1.2)	25.3 (0.5)	44.3 (1.1)
Nonane	40.3 (0.6)	62.1 (1.7)	31.7 (0.8)	56.7 (1.4)	29.6 (0.2)	56.7 (0.2)
2-Methylhexane	31.5 (0.3)	51.5 (0.6)	24.9 (1.6)	58.7 (1.5)	17.8 (1.2)	40.6 (1.0)
3-Methylhexane	31.8 (0.3)	51.7 (0.7)	26.8 (2.3)	63.3 (1.6)	19.4 (0.6)	42.1 (0.4)
2,3-Dimethylpentane	31.4 (0.2)	51.0 (0.3)	24.9 (1.9)	59.9 (1.8)	20.2 (2.5)	50.8 (2.2)
2,4-Dimethylpentane	30.2 (0.1)	50.1 (0.3)	23.5 (1.8)	58.3 (1.7)	18.3 (1.4)	45.9 (1.2)
2,2,3-Trimethylbutane	29.8 (0.2)	48.3 (0.3)	23.4 (1.6)	52.8 (2.3)	17.6 (4.3)	51.8 (1.2)
Cyclohexane	29.1 (0.2)	44.6 (0.3)	22.8 (0.9)	53.4 (0.9)	29.0 (0.0)	63.0 (1.1)
Benzene	29.4 (0.3)	45.3 (0.8)	28.8 (0.7)	61.7 (0.9)	25.3 (0.7)	56.3 (1.0)
Toluene	33.5 (0.3)	50.4 (0.8)	32.2 (0.7)	64.1 (1.0)	28.5 (0.4)	58.2 (0.8)
Ethylbenzene	37.9 (0.5)	57.5 (1.3)	34.5 (0.7)	64.1 (1.4)	30.2 (0.5)	58.9 (1.2)
o-Xylene	35.8 (0.8)	49.9 (3.2)	36.3 (0.8)	65.3 (1.6)	32.2 (0.5)	60.1 (0.9)
m-Xylene	35.3 (0.6)	49.9 (2.4)	31.4 (0.3)	57.6 (0.3)	31.8 (0.4)	57.5 (0.4)
p-Xylene	35.5 (0.7)	50.2 (2.5)	35.2 (0.8)	67.8 (0.7)	31.5 (0.6)	54.9 (0.5)